OncoTargets and Therapy

Dovepress
open access to scientific and medical research

Open Access Full Text Article

ORIGINAL RESEARCH

RETRACTED ARTICLE: Identification of Osteosarcoma Metastasis-Associated Gene Biomarkers and Potentially Targeted Drugs Based on Bioinformatic and Experimental Analysis

This article was published in the following Dove Press journal:
OncoTargets and Therapy

Ming-De Cao[1]
Yan-Cheng Song[2]
Zhong-Meng Yang[1]
Da-Wei Wang[1]
Yi-Ming Lin[1]
Hua-Ding Lu[1]

[1]Department of Orthopaedics, The Fifth Affiliated Hospital of Sun Yat-Sen University, Zhuhai 519000, Guangdong, People's Republic of China; [2]Department of Orthopedics, The First Affiliated Hospital of Guangdong Pharmaceutical University, Guangzhou 510000, Guangdong, People's Republic of China

Background: Metastasis is the leading cause of death for patients with osteosarcoma (OS). In the present study, we explore the biomarkers for metastatic OS and provide potential therapeutic approaches.

Materials and Methods: RNA-Seq data and clinical follow-up information were downloaded from TARGET and GEO databases. A Cox regression model was used to analyze metastatic events. L1000FWD, DGIdb, and CMap databases were used to identify potential drugs related to metastasis. Invasion and migration transwell assays and an adhesion assay were used to identify biological function of genes.

Results: A total of 5 metastasis-related signatures (MRSs) were associated with the prognosis based on the TARGET or GSE21257 cohorts, among which *IL10RA* and *TLR7* genes were especially significant. In the DGIdb drug–gene interaction database, *TLR7* and *IFNAR1* were found to have potential interactions with drugs. After inhibiting the expression of *TLR7*, the migration, invasion, and adhesion ability of OS cells were significantly enhanced, which further promoted metastasis.

Conclusion: We identified a set of MRS that may be related to OS metastases. Among them, *TLR7* plays a vital role and may be a potential target for OS metastasis treatment.

Keywords: osteosarcoma, metastatic-related signatures, drug–gene interaction, TLR7, migration, invasion

Introduction

As one of the most common primary mesenchymal malignancies, osteosarcoma (OS) is characterized by the direct differentiation of malignantly proliferating tumor cells into bone or bone-like tissue.[1] OS mainly occurs in children and adolescents and shows a strong male predominance. With a high degree of malignancy, OS usually progresses rapidly.[2] For decades, new comprehensive treatments, such as the combination of tumor resection and neoadjuvant chemotherapy, have been widely used in clinical treatment, leading to improved survival prognosis.[3,4] However, such treatments cannot completely inhibit the growth of tumors, and the mortality rate of OS patients remains high.[5] Therefore, it is critical to explore new biomarkers of OS to provide a solid theoretical basis for new treatment methods, thereby improving the often bleak prognosis of patients with OS.

Correspondence: Hua-Ding Lu
Department of Orthopaedics, The Fifth Affiliated Hospital of Sun Yat-Sen University, Zhuhai 519000, Guangdong, People's Republic of China
Tel +86 13807918420
Email johnniehuading@163.com

submit your manuscript | www.dovepress.com
DovePress
http://doi.org/10.2147/OTT.S256617

Due to the prominent metastatic characteristics and high invasiveness of OS, by the time of diagnosis, the lesion has metastasized in 10–20% of OS-bearing patients. In addition, with a recurrence rate of as high as 80%, lung metastasis is the most common route of systemic recurrence in OS patients.[6] Despite the improvements in surgical and adjuvant radiotherapy, the five-year survival rate of patients with metastatic or recurrent OS has not increased considerably over time and remains at approximately 20%,[7–9] significantly lower than that of patients without pulmonary metastases.[10,11] Recently, researchers have attempted to explore the mechanism of OS metastasis and identify the biomarkers for early diagnosis and metastasis prediction. For example, Wnt/β-catenin[12–14] and hypoxia-associated pathways[15] have demonstrated involvement in distal OS metastasis. In addition, a growing body of evidence suggests that non-coding RNAs,[6] including miRNA,[16] lncRNA,[17] and CircRNA,[18] are involved in metastasis and associated with poor OS prognosis. Investigators have confirmed the predictive effect of the miRNAs miR-27a and miR-181c on metastasis.[19] However, these indicators are not suitable for early clinical diagnosis due to low specificity and lack of definitive clinical evidence. Therefore, it is critical to discover accurate biomarkers of OS metastasis, thereby providing a reliable basis for the development of novel effective therapeutic targets to curb the occurrence of metastasis and reduce the mortality rate.

With the development of gene microarray and high-throughput next-generation sequencing, bioinformatics analysis of gene expression profiling has been broadly applied to explore the mechanism underlying diseases and potential diagnostic biomarkers or treatment targets. Several studies have used bioinformatics to screen biomarkers of OS patients. Jing[20] comprehensively analyzed GSE66673, GSE49003, and GSE3758 cohorts to identify candidate pathogenic genes of OS, and used GO and KEGG enrichment analysis to predict the functional annotation and potential pathways of differentially expressed genes (DEGs). The author established an OS-specific transcriptional regulatory network was established to study TF targeting of DEG. Wu et al[21] constructed a risk score model based on eight genes for predicting overall survival of OS patients. Sun[22] used the significance analysis of microarray (SAM) method, integrating GSE21257, GSE9508, GSE49003, and GSE66673 cohorts to identify differentially expressed genes and analyze differentially expressed pathways for metastatic and non-metastatic OS based on the support vector machine (SVM) model. However, most of these studies have been limited only to data analysis without rigorous experimental validation on specific OS metastasis genes. In addition, they have not explored the relationship between genes and pharmacology.

In the present study, a set of metastasis-related signatures (MRSs) associated with OS patients was identified by integrating different cohorts. Functional and potential drugs related to the metastasis mechanism of OS were explored, which may assist in the mining of potential drugs as new alternatives for the treatment of OS. In addition, the function of the TLR7 gene was comprehensively validated. Our research will provide a better understanding of OS metastasis and provide pathways to novel, effective treatments.

Materials and Methods

Data Download and Preprocessing

The latest clinical information and gene expression profile of OS were downloaded from TARGET, which contained a total of 89 samples. GSE21257, GSE32981, GSE39055, and GSE49003, which contained 53, 23, 37, and 12 tumor samples or cell lines, respectively, were downloaded from the GEO database.

The OS data downloaded from TARGET were pretreated by removing 1) samples devoid of clinical information or have a total survival time of fewer than 30 days, 2) data of normal tissue samples, and 3) genes demonstrating zero expression level in more than half of the samples.

GEO data were pretreated by 1) removing the data of normal tissue samples, leaving only the data of tumor tissue; 2) converting the total survival time in years or months into days; 3) mapping the chip probe into human gene SYMBOL using the bio-conductor package.

MRS Filtering and Feature Annotations

As TARGET, GSE21257, GSE39055, and GSE49003 are chip-encoded data, the downloaded expression profile data were normalized. We conducted the DEG analysis through the R software limma package (https://bioconductor.org/packages/limma/) on metastasis and non-metastasis group samples. Given that the number of DEGs of TARGET and GSE32981 data is extremely small, $p<0.01$ and $|\log_2$ fold change$|>0.5$ were set as the threshold. As for GSE21257 and GSE49003 data, FDR<0.05 and |log2 fold change|>0.5 were taken as the threshold. DEGs obtained from the four cohorts were defined as MRSs.

We used clusterProfiler package (https://bioconductor.org/packages/clusterProfiler/) to perform functional enrichment analysis of all GO terms, and we conducted Reactome pathway analysis through WebGestalt, R package (https://github.com/bzhanglab/WebGestaltR). FDR<0.05 was assigned as the threshold for significant enrichment.

Prognosis Analysis

A univariable Cox regression model was used to analyze the prognostic relationship between MRSs and metastatic events. Considering the low (85/53) numbers of the TARGET and GSE21257 cohort samples with prognostic information, we set log-rank p<0.1 as the significance threshold. Kaplan-Meier analysis was used through the R software survival package (https://bioconductor.org/packages/survcomp/) to plot the overall survival. Unless otherwise stated, *** indicates p<1e-5, ** indicates p<0.01, and * indicates p<0.05.

Mining of Potential Drugs

The L1000FWD tool (http://amp.pharm.mssm.edu/l1000fwd/)[23] was used to identify the small molecules related to DEGs. L1000 database records the aberrantly up-regulated or down-regulated genes induced by more than 16,000 drugs or small molecules in cancer cell lines. By comparing identified DEGs with those genes recorded in the database, we can reversely deduce the relevant small molecule. In the results of the annotated L1000FWD, if the gene sets provided by us were consistent with those gene sets recorded in the database, then the small molecule corresponding to such set was defined as similar; if not consistent, it were defined as the opposite.

The DGIdb (http://www.dgidb.org) database[24] records the interaction information of more than 40,000 genes and 10,000 drugs. Unlike the L1000 database, DGIdb records the correlative information between specific genes and their interacting drugs. Based on the gene information provided by the user, the drug that interacts with the selected gene will be identified.

The four subtypes of MRS gene symbols were converted to Affymetrix probe IDs using the Bioconductor R package, prior to querying using CMap (http://portals.broadinstitute.org/cmap/).[25] In the CMap database, drugs with significantly negative scores are predicted to be new therapeutic medications for OS. CMap uses an algorithm of GSEA (gene set enrichment analysis) to calculate the correlation coefficient. An average coefficient of no greater than 0.65 could be used to identify potential drug candidates. For gene probes provided by CMap, an amplitude of ≤−0.67 or >0.67 was reserved for those significantly aberrantly expressed, which could be used for pathway analysis; an amplitude of ± 0.67 represents a two-fold change between the treatment and the control.

Migration, Invasion, Wound-Healing Assay

MG-63 cells were purchased from the Type Culture Collection China Centre. DMEM/F12 containing 10% FBS was used to culture cells in an incubator with 37°C and 5% CO2 atmosphere. We investigated the migration and invasion of MG-63 cells using transwell chambers (Corning, MA, USA) in a 24-well plate containing 8-μm pore. Serum-free tumor cells in F12/DMEM were placed in the upper chamber, and F12/DMEM containing 10% FBS was placed in the lower chamber. We used an upper chamber that had been pretreated with Matrigel coating (2mg/mL) for the invasion assay, and an untreated upper chamber for the migration assay. After culturing for 24h, the cells that had migrated towards or invaded the lower chamber were fixed with 4% paraformaldehyde for 30min, stained with crystal violet, and counted by bright-field microscopy. We grew tumor cells to 95% confluence in DMEM without FBS overnight for the wound-healing closure assay. We scratched the monolayer of cells using a sterile 10μL pipette tip, and the cells were cultivated for 24h.

Lentiviral RNAi Cell Transduction

Lentiviral vectors containing human TLR7 or non-target shRNA were obtained from Sigma, packaged into recombinant lentivirus, and stably expressed in OS cells as described previously.[26] The transduction efficiency was evaluated by flow cytometry.

Animal Experiments

We bred BALB/c (nu/nu) mice under specific pathogen-free (SPF) conditions in the Animal Research Center, and mice six-weeks-old were used in experiments. For the in vivo lung metastasis model, MG-63-GFP cells with or without CC-CAFs were injected at a density of 1×10^6 in 100μL PBS via the tail veins of the randomized mice (n=7 per group). After three weeks, the mice were sacrificed, and the metastatic sites within the lungs were isolated. Metastatic tumor fragments were minced into 1-mm cubes and digested in collagenase IV (Invitrogen, CA, USA) for 3h at 37°C. Digested cells were washed twice with complete cell culture media and transferred into RPMI1640 (Invitrogen, CA, USA) containing 10% FBS and 1% penicillin/streptomycin and 1 μg/mL

puromycin to eliminate all except MG-63-GFP cells derived from the metastatic lung site. After the selection process, the cells were analyzed by flow cytometry and Western blotting.

Static Adhesion Assay

HUVECs were seeded onto 6-well plates at a density of 5 × 104 cells/well. Stably transfected MG-63 cells with GFP were plated (5 × 104 cells/well) and incubated for 30min at 37°C. The unattached cells were gently washed twice with 10% FBS-containing DMEM, and tumor cells adhered to HUVECs were counted under fluorescence microscopy.

Statistical Analysis

After RMA normalization, limma was applied to perform differential analysis. The genes with differential analysis results of "FDR< 0.1" were defined as DEGs. Log-rank $p<0.05$ was chosen as significant. The version of R was 3.5.1. All data are the results of 3 independent experiments, expressed as mean ± standard deviation (± s).

Results

Sample Information Statistics

The pre-processed OS cohorts are listed in Table 1. A total of 209 samples were obtained, of which 85 satisfied the criteria of conditional samples in TARGET: 53 samples in GSE21257, 23 samples in GSE32981, 12 samples in GSE39055, and 36 samples in GSE49003 met the standard. Among them, TARGET, GSE21257, GSE32981, and GSE49003 cohorts have both metastatic and non-metastatic sample information, which were used to identify DEGs. The TARGET and GSE21257 cohorts have overall survival time, while the GSE39055 cohort has recurrence prognosis, all data used to evaluate the prognostic value of DEGs. The overall survival between metastatic and non-metastatic patients in TARGET and GSE21257 cohorts were significantly different (Figure 1A and B). The overall survival of non-metastatic samples was also significantly better than that of metastatic samples (Figure 1C and D).

Identification of MRS and Functional Analysis

Integrating TARGET, GSE21257, GSE32981, and GSE49003 cohorts, we analyzed the DEGs of metastatic and non-metastatic samples. DEGs obtained from 4 cohorts are defined as MRS. The number of up-regulated MRSs was larger than down-regulated MRSs in non-metastatic samples (Table 2, Figure 2A-C), suggesting that metastasis is more likely to involve the inhibition, rather than the activation, of specific pathways. Since the GSE49003 cohort contains cell lines with or without metastatic ability, it is reasonable to speculate that this may lead to a large difference between the MRSs identified by GSE49003 and those identified by TARGET, GSE21257, and GSE32981 (Figure 2D).

Table 1 Research Cohorts Statistics

	TARGET	GSE21257	GSE32981	GSE49003	GSE39055
Event					
Alive	55	30			18 (Non-recurrence)
Dead	30	23			18 (Recurrence)
Gender					
Female	7	19	10		17
Male	48	34	13		19
DiseaseAtDiagnosis					
Metastatic	22	34	11	6	
Non	63	19	12	6	
Age					
Median	14.09	16.67	18		11
Mean	14.8	18.71	21.35		13.5
Overall Survival (mean days)*		*			*
Alive	1787.9	2755			2152
Dead	894.4	1145			1111.7

Notes: GSE49003 refers to four osteosarcoma cell line, of which KHOS and KRIB are metastatic types, and HOS and U2OS are non-metastatic types. *Indicates a significant difference in overall survival time (OS).

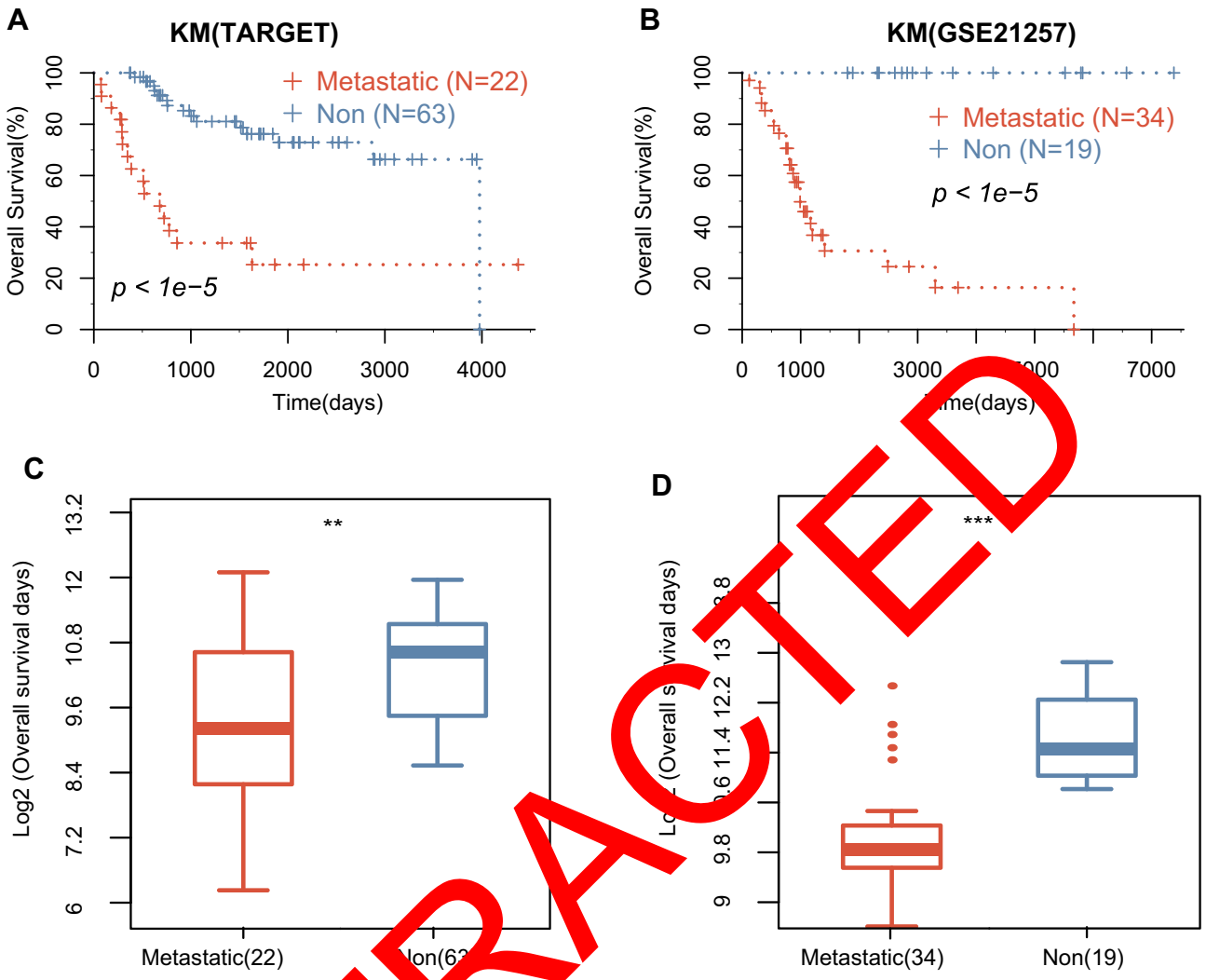

Figure 1 The prognostic overall survival time between metastatic and non-metastatic samples. (**A** and **B**). Kaplan–Meier survival curve of the metastatic and non-metastatic groups in TARGET and GSE21257 cohorts. (**C** and **D**). Comparison of overall survival time (OS) between the metastatic and non-metastatic groups in TARGET and GSE21257 cohorts. **Represents P value <0.05, ***Represents P value <0.01.

We further compared the overlapping MRSs in 4 cohorts and found very few overlapped among all cohorts (shared/total MRSs: 1/1377, Figure 3A). This result seems to reflect a wide range of heterogeneity with respect to the metastatic capacity of OS. Although the number of overlapped MRSs is small, these MRSs were significantly enriched in immune-related GO terms (Figure 3B-E). From the point of gene expression level, immune-related genes are generally down-regulated in the metastasis group: it is speculated that the inhibition of the immune system may contribute to the metastasis of OS.

Table Statistics of MRS in Different Cohorts

MRS	Non/Met	
TARGET	Up Down	32 25
GSE21257	Up Down	178 35
GSE32981	Up Down	121 121
GSE49003	Up Down	395 470

Notes: "Non" indicates non-metastatic, and "Met" indicates metastatic.

The results of the Reactome pathway analysis showed that the GSE21257 cohort was significantly enriched in neutrophil degranulation, costimulation by the CD28 family, PD-1 signaling, chemokine receptors binding chemokines, and other pathways (S1_FigA). The GSE32981 cohort was significantly enriched in pathways such as surfactant metabolism, interleukin-10 signaling, regulation of TLR by endogenous ligands, and chemokine receptors

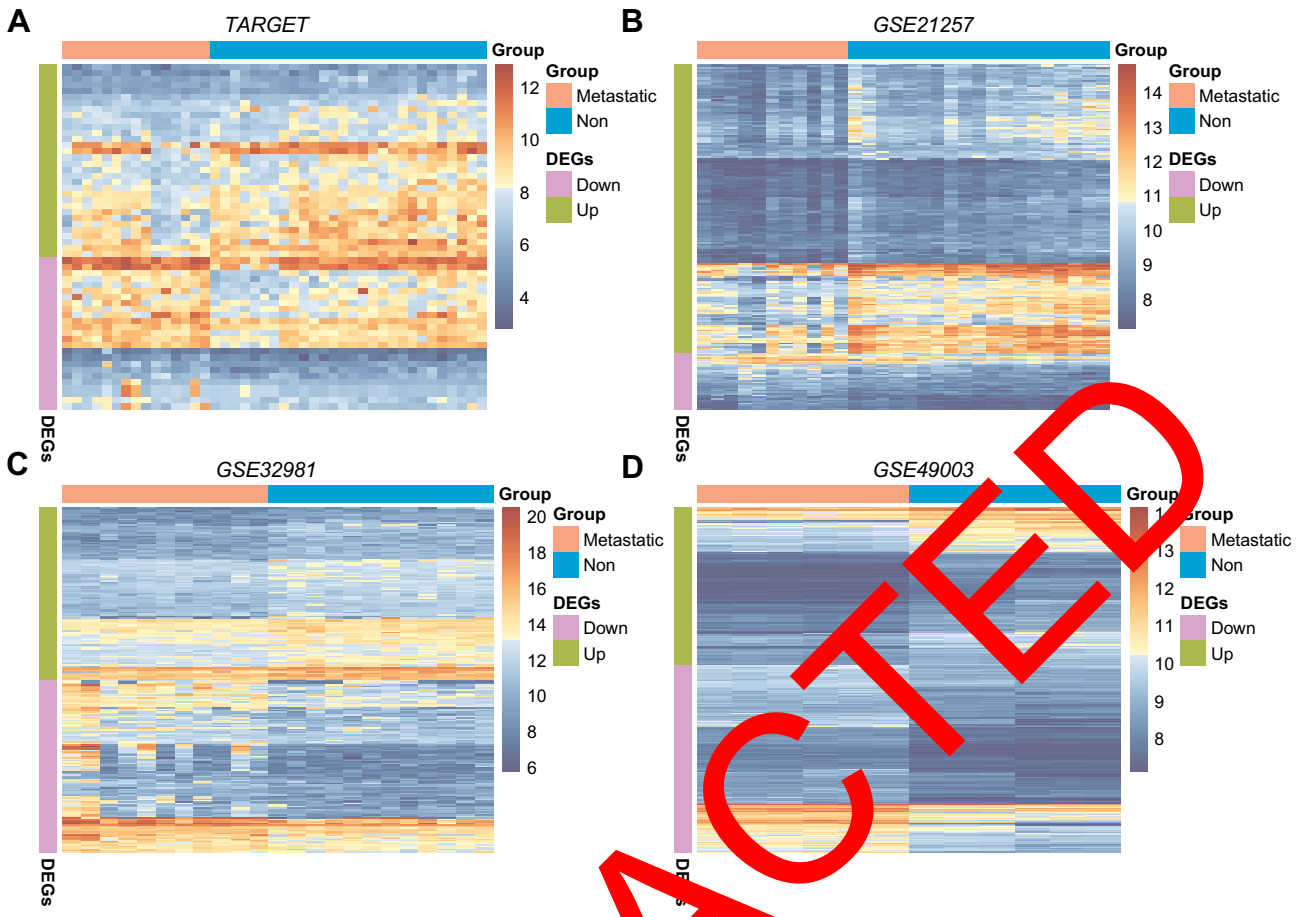

Figure 2 MRS screening and functional analysis. (**A**) Expression level of DEGs in metastatic and non-metastatic groups of TARGET cohort; (**B**) expression level of DEGs in metastasis and non-metastatic groups of the GSE21257 cohort; (**C**) expression level of DEGs in metastatic and non-metastatic groups of GSE32981 cohort; (**D**) GSE49003 cohort transfer and expression levels of non-metastatic cell lines DEGs.

binding chemokines (S1 FigB). Among the 15 MRSs obtained from TARGET and the GSE49003 cohort were not significantly enriched Reactome pathway (FDR>0.05)

Correlation Between MRSs and Prognosis

Because the GSE49003 cohort has the most identified MRSs, and the TARGET and GSE21257 cohorts had prognostic information, to include more prognostic MRSs, we integrated MRSs of GSE49003, TARGET, and GSE21257 using univariable Cox regression to identify 15 prognostic MRSs (Table 3).

These genes were divided into adverse prognostic factors with HR (hazard ratio)>1, and favorable prognostic factors with HR<1. The favorable prognostic MRSs were down-regulated in the metastatic group, whereas the unfavorable prognostic MRSs were up-regulated in the metastatic group (Table 3). In the TARGET and GSE21257 cohort, *IL10RA* and *TLR7* genes were significantly associated with the prognosis.

TARGET, GSE21257, and GSE39055 cohorts were used to perform survival analysis to identify the overall survival and recurrence value of *IL10RA* and *TLR7* genes. The cohorts were subdivided into high expression group (L2) and low expression group (L1), according to the median expression level of *IL10RA* and *TLR7*. The results showed the overall survival of the L2 group was better than that of the L1 group; among them, the survival of *TLR7* in TARGET was marginally significant (Figure 4A-D).

There was no significant recurrence between the two groups in the GSE39055 cohort. We speculated that this is due, to a certain extent, to the small sample size of GSE39005 (S2 Fig).

Analysis of Potential Drugs for Metastasis-Related Signatures

The L1000 database provides the gene expression profiles induced by more than 16,000 drugs and small molecules

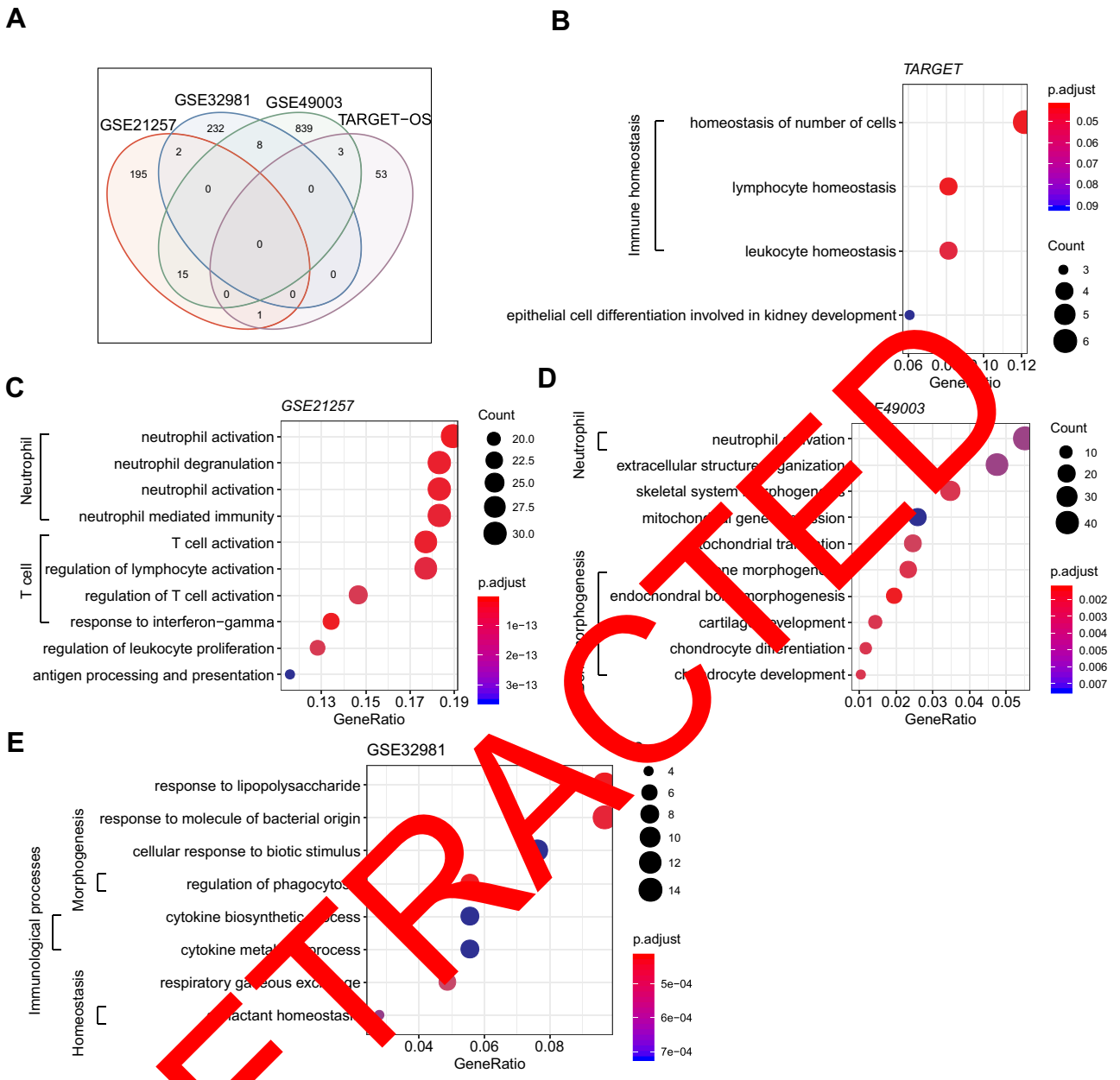

Figure 3 MRS co on of m stasis and -transfer OS subtypes and functional annotation. (**A**) MRS intersections shared by 4 cohorts; functional enrichment bubble map of MRSs i (**B**) TA ET, (**C**) E21 and (**D**) GSE49003; (**E**) pathway enrichment bubble map of MRSs in GSE32981.

on appro ely 1000 tumor cell lines. We used the L1000FWD l to conduct a reverse database search of the up- and down-regulated MRS in TARGET, GSE21257, GSE32981, and GSE49003 cohorts, and obtained 51, 15, 92, and 64 small molecule drug candidates, respectively. The number of small molecular substances found in all four cohorts was minimal, which may be attributed to the extremely low number of MRSs. In addition, we found a small compound, BRD-A15079084, which appeared in all three cohorts, suggesting it as a potential drug candidate (Figure 5A).

In the DGIdb (Drug–Gene Interaction Database), we analyzed 15 potentially interacting drugs with MRSs that were significantly associated with prognosis and found that two genes, *TLR7* and *IFNGR1*, can potentially interact with drugs (S1_Table). These drugs interact with genes to induce their expression (Figure 5B). Considering that *TLR7* is a favorable prognostic factor, its expression is inhibited in the metastatic group. Therefore, these drugs that can promote *TLR7* gene expression may play a specific role in the clinical intervention of metastatic OS. TLR7 was chosen for further experimental research.

Table 3 HR and p value for 15 Prognostic MRS

gName	TARGET			GSE21257			GSE49003
	HR	Log Rank p	DEGs p	HR	Log Rank p	DEGs padj	DEGs padj
FRAS1	0.658	0.006	0.009↓			0.950	<0.001↓
TNFRSF21	0.518	0.009	0.006↓			0.830	<0.001↑
IL10RA	0.501	0.007	0.076	0.535	0.031	0.031↓	0.0133↑
TLR7	0.633	0.024	0.007↓	0.592	0.008	0.005↓	0.8578
TM4SF1	0.675	0.047	0.966			0.206	<0.001↑
PLOD2	1.540	0.055	0.009↑			0.612	0.0397↓
LPXN	0.613	0.068	0.207			0.022↓	<0.001↑
EBI3	0.398	0.095	0.003			0.028↓	0.0010↓
LCP2	0.658	0.096	0.123			0.019↓	0.8945
CXCL16			0.085	0.418	0.009	0.0[illegible]	0.001↓
SPINT2			0.021	0.590	0.031	0.019↓	0.[illegible]519
PEA15			0.565	0.398	0.034	0.011↓	0.0080↓
IFNGR1			0.252	0.501	0.038	0.03[illegible]↓	0.0017↓
LITAF			0.767	0.471	0.066	0.[illegible]03↓	0.0018↓
GPSM3			0.700	0.552	0.069	0.016↓	0.0003↑

Notes: DEGs p marked in red indicates a significant different expression between metastatic and non-metastatic group. ↓ indicates down-regulation in the metastatic group, while ↑ indicates up-regulation in the metastatic group.

In the CMap database, we observed that fewer drugs were commonly found in the four cohorts (Figure 5C, S2_Table). However, viomycin, a high basic peptide secreted by Streptomyces, is annotated in all four cohorts. Viomycin is a compound that inhibits protein synthesis and is used to treat tuberculosis. In addition, 12 other drugs, including diphenine, alexidine, camptothecin, CP-320,650-01, digoxigenin, genistein, GW-8510, H-7, iopamidol, nadolol, PD-[illegible]691, and sulfamonomethoxine appeared in at least three data sets. Although these potential drug candidates have been widely used in clinical practice, further research is needed to ascertain their possible use in treating other diseases.

Experiments on the Biological Behavior of TLR7

We used Western blot to investigate the basal expression of TLR7 in four OS cell lines and found that MG-63 and Saos-2 expressed the most TLR7 and were thus used for subsequent study (Figure 6A). After transfection of shRNA targeting TLR7, transduction efficiency was confirmed by flow cytometry (Figure 6B). As shown in Western blot results, the effect of shRNA-based knockdown was studied, and #2 shRNA was used for subsequent study (Figure 6C). Transwell migration and invasion assays were performed to evaluate function of TLR7 expression on migration and invasion. After TLR7 was down-regulated, migration and invasion were enhanced significantly. Results of the wound-healing assay further confirmed this result. As expected, migration of cells increased when TLR7 was knocked down in MG-63 and Saos-2 (Figure 6D-F). As shown in the results of the adhesion assay (Figure 6G), the adhesion of MG-63 OS cells to endothelial cells increased as TLR7 was down-regulated, a result confirmed in the Saos-2 cell line. To further support the underlying role played by TLR7 in vivo, MG-63 was used to construct a lung metastasis model, and after three weeks, tumor cells at the metastasis site were isolated and designated as MG-63-MS (metastasis site). TLR7 in MG-63-MS and MG-63 was evaluated by Western blot. As shown in Figure 6H, MG-63-MS expressed lower TLR7 than MG-63, indicating that down-regulation of TLR7 is associated with increased metastasis potential.

Discussion

Osteosarcoma is a highly malignant bone tumor with high metastatic potential: metastasis (most commonly, of the lung[27,28]), has already occurred for 10–20% of the patients at the time of diagnosis. The onset and progression of tumors is a complex process, and the proliferation and metastasis of OS cells are regulated by numerous factors. Hence, elucidating the proliferation and metastasis mechanisms of OS is an important approach to identify

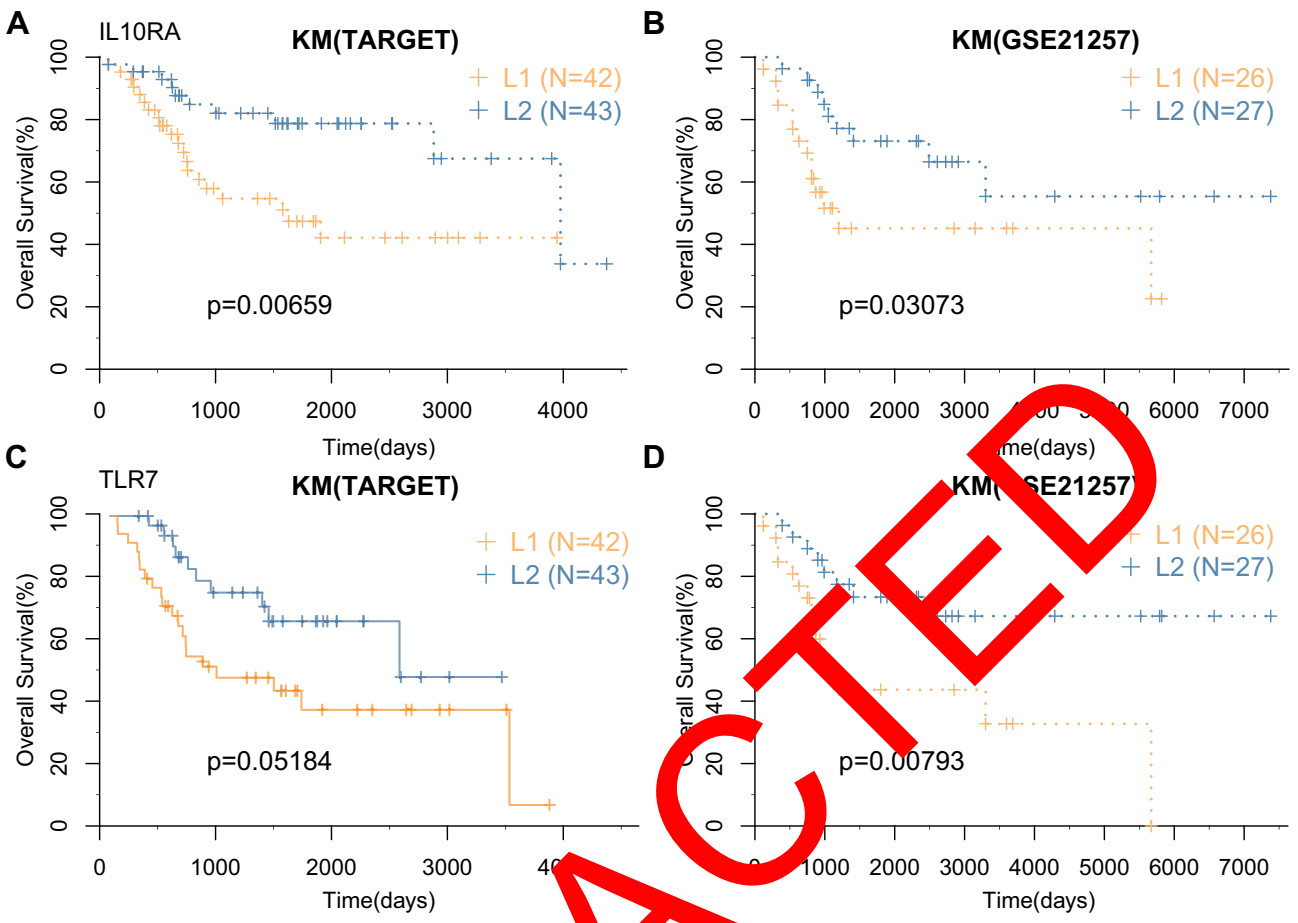

Figure 4 Correlation between MRSs and prognosis. (**A** and **B**) Prognostic KM curve of IL10RA gene in high and low expression groups in TARGET and GSE21257 cohorts; (**C** and **D**) prognostic KM curve of TLR7 gene in high and low expression groups in TARGET and GSE21257 cohort.

the biomarkers for early diagnosis and to assess OS occurrence and metastasis.

Recently, although much research has focused on the metastasis of OS, the tumor biomarkers for early prediction of metastasis remain scarce. In-depth studies on the molecular mechanisms of metastasis to identify effective, sensitive, and specific OS metastasis molecular markers, among many other factors, are vital to improving the prognosis of patients with OS.[29,30] In the current study, we collected data from TARGET and GEO databases. The prognosis survival time of the patients in the metastatic group was significantly lower than that in the non-metastatic group, indicating that metastasis is a significant factor affecting the prognosis of patients.

In screening metastasis-related signatures (MRSs), we found that few MRSs were annotated in different cohorts, indicating the significant heterogeneity of OS. Gene Ontology annotations yielded a common result that MRSs were significantly enriched in "immune". Based on the above results, we suggest that inhibition of the immune system may be involved in the metastasis of OS, shedding light on the novel approach of immunotherapy to realize the targeted inhibition of OS metastasis.

Currently, the comprehensive treatment of OS mainly relies on surgery and postoperative chemotherapy therapies with MAP (methotrexate, doxorubicin, and cisplatin), which enhance the 5-year survival rate of patients to approximately 60%.[31,32] However, the prognosis of patients with metastatic OS remain unfavorable, mostly due to the resistance or even unresponsiveness to currently used chemotherapy regimens. In recent years, with the continuous advancement and development of targeted therapy for tumors, targeted drugs have demonstrated great therapeutic potential in various OS models, suggesting that targeted therapy may be a promising approach for patients with metastatic OS.[33]

In this study, we attempted to reverse-search the MRSs in the L1000, DGIdb, and CMap databases. In the L1000

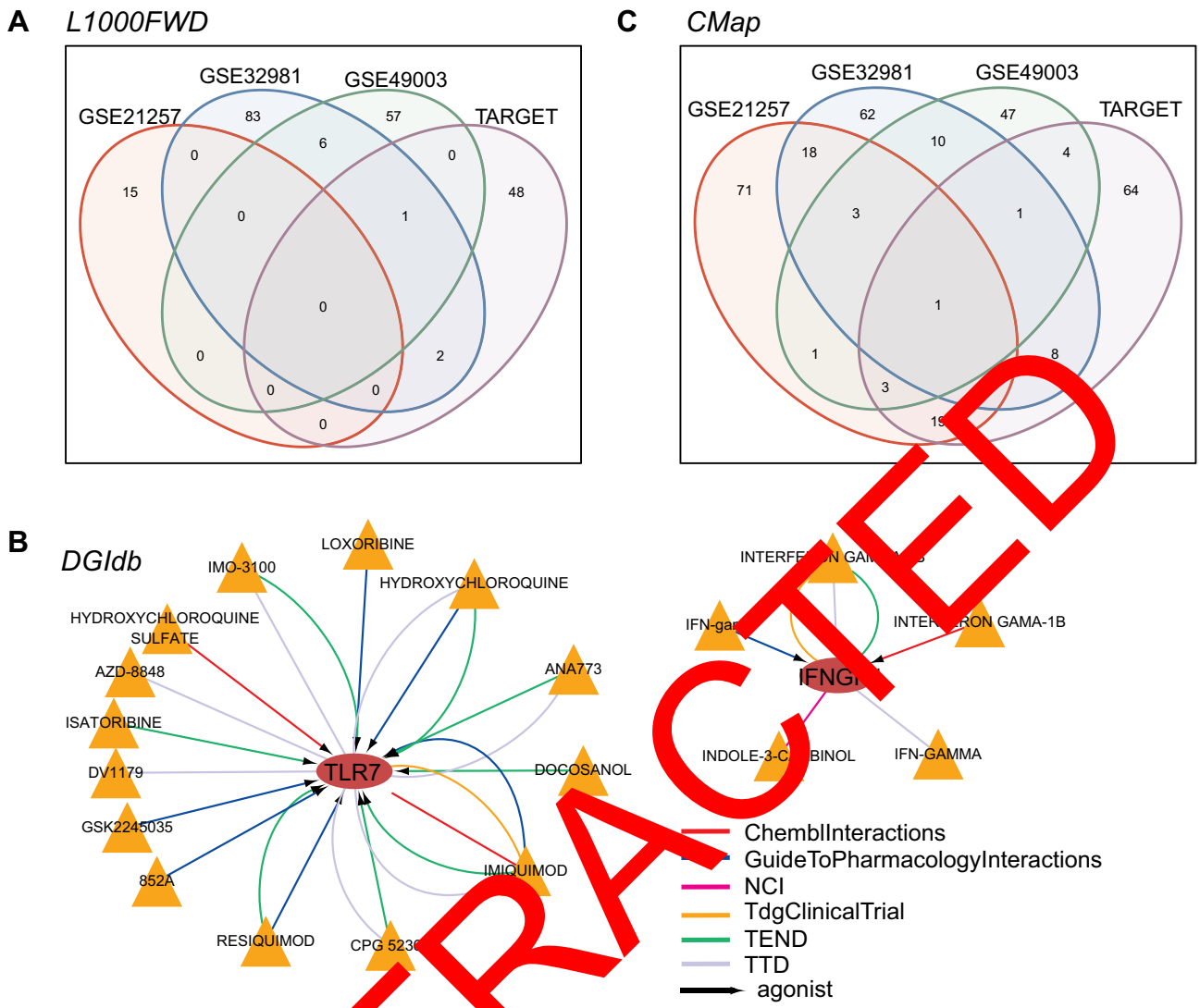

Figure 5 Data mining of potential drugs of MRS. (**A**) L1000 database annotation of four cohorts; (**B**) DGIdb database annotation of 15 MRSs; (**C**) CMap database annotations of four data sets. Circle in Figure 5B indicates gene, triangle represents the small molecule, arrow represents the agonist relationship between the gene and the small molecule, and the color of the line suggests the different sources of interaction databases.

database, we identified the potential clinical value of the small molecule SRD-A1507284. In the DGIdb database, we identified potential interactions between TLR7 and IFNGR1 for 5 MRSs. Given that TLR7 is a protective factor, and its expression level is down-regulated in the metastatic group, targeting TLR7 may be a new measure for treatment. To further confirm our findings, we performed relevant molecular biological validation on TLR7. The results showed that after inhibiting the expression of TLR7, the migration and invasion ability of OS cells was significantly enhanced. With the down-regulation of TLR7 expression, the adhesion between OS and endothelial cells increased, which further promoted metastasis. The lung metastasis model further confirmed that the down-regulation of TLR7 is associated with an increase in metastatic potential.

Finally, as shown in the CMap database, viomycin was commonly annotated among the differential MRS in all four cohorts. Viomycin is a strong basic peptide produced by Streptomyces and a compound that inhibits protein synthesis. It is currently mainly used for the treatment of tuberculosis, and its anti-tumor effect has not been previously mentioned in relevant studies.[34,35] We speculate that viomycin may be used for the targeted treatment of patients with metastatic OS. Taken together, we identified a series of drugs that interact with MRSs through reverse screening, providing more potential options for the treatment of patients with metastatic OS.

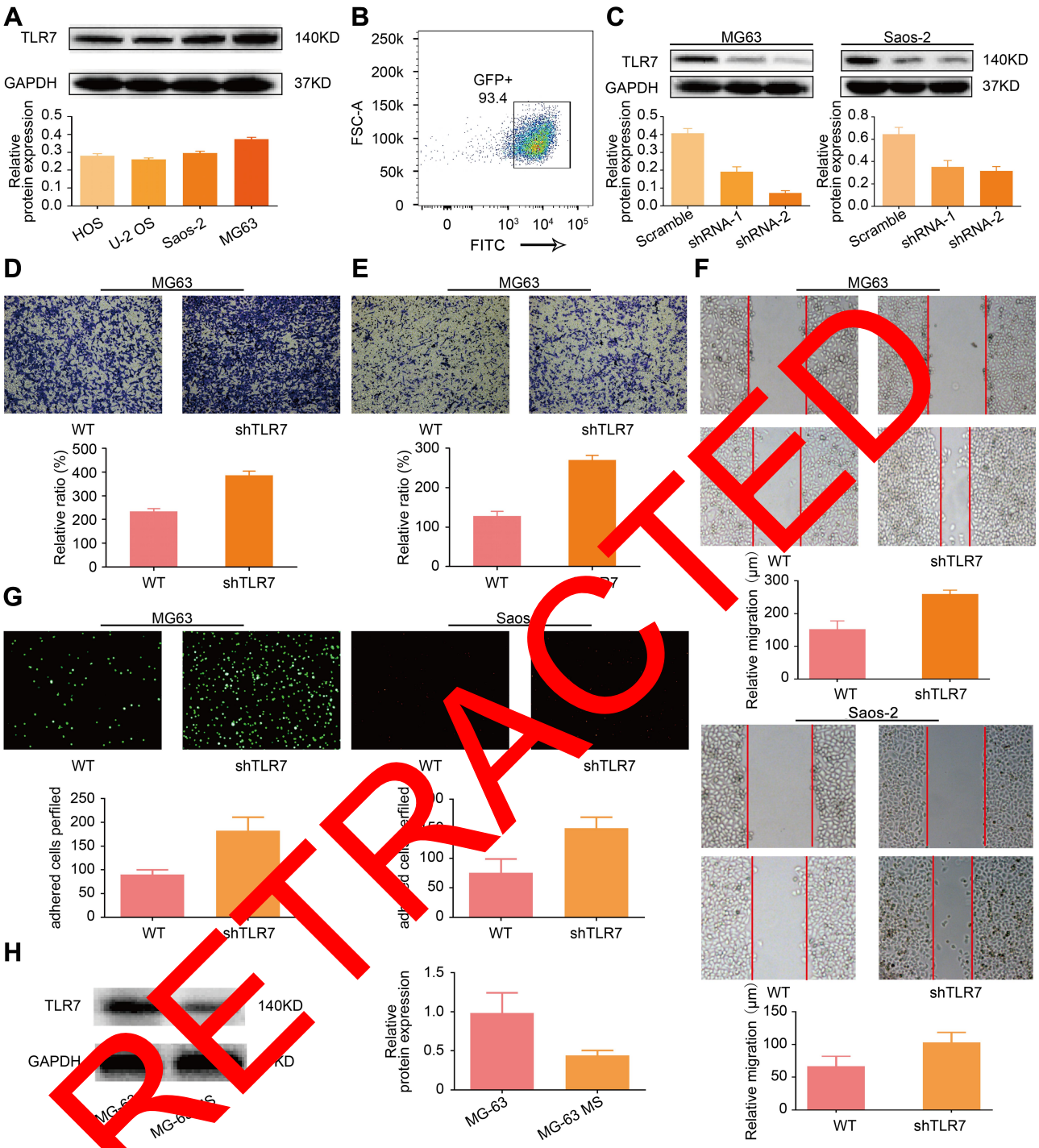

Figure 6 Inhibition of TLR7 expression can promote OS cell metastasis. (**A**) Basal expression of TLR7 in 4 kinds of OS cell line; (**B**) transduction efficiency confirmation by flow cytometry; (**C**) transfection efficiency of shRNA targeting TLR7 in MG-63 and Saos-2 by Western blot; (**D** and **E**). Transwell-based invasion and migration of TLR7 in MG-63. (**F**) Wound-healing assay of TLR7 in MG-63 and Saos-2; (**G**) function of TLR7 on cell adhesion assay in MG-63 and Saos-2; (**H**) lung metastasis model constructed to evaluate metastasis potential of TLR7.

Conclusion

In this research, TARGET and GEO cohorts were used to identify a set of MRSs related to OS. We also mined the potential functions and drugs of MRSs to understand the etiology and metastasis mechanism further. For the core MRS—TLR7—we conducted a series of experiments in vivo and in vitro, and the results were consistent with the data analysis. TLR7 plays a vital role and may be a potential target for metastatic OS treatment.

Data Sharing Statement

The data used to support the findings of this study are available from the corresponding author on reasonable request.

Ethics Approval and Consent to Participate

All the source of cell lines were purchased from the Type Culture Collection China Centre. Animal assays were performed according to Guangdong Experimental Animal Care Guideline. All experiments were approved by the Ethics Committee of Sun Yat-Sen University institution.

Acknowledgments

The authors thank the numerous individuals who participated in this study.

Author Contributions

Ming-De Cao made substantial contributions to conception and design, Ming-De Cao, Yan-Cheng Song, Da-Wei Wang and Yi-Ming Lin were the major contributor in writing the manuscript. Zhong-Meng Yang was involved in cell experiments and data analysis. Hua-Ding Lu guided research and provided financial support. All authors contributed to data analysis, drafting or revising the article, have agreed on the journal to which the article will be submitted, gave final approval of the version to be published, and agree to be accountable for all aspects of the work.

Funding

This study was supported by National Natural Science Foundation of China (81572674, 81772384); Natural Science Foundation of Guangxi Autonomous Region (No. XZ2018ZRG-177); Zhuhai medical and health science and technology plan project P.R. China (No. 20171009E0302).

Disclosure

The authors report no conflicts of interest for this work.

References

1. Luetke A, Meyers PA, Lewis I, Juergens H. Osteosarcoma treatment – where do we stand? A state of the art review. *Cancer Treat Rev*. 2014;40(4):523–532. doi:10.1016/j.ctrv.2013.11.006
2. Saraf AJ, Fenger JM, Roberts RD. Osteosarcoma: accelerating progress makes for a hopeful future. *Front Oncol*. 2018;8:4. doi:10.3389/fonc.2018.00004
3. Carina V, Costa V, Sartori M, et al. Adjuvant biophysical therapies in osteosarcoma. *Cancers (Basel)*. 2019;11(3):348. doi:10.3390/cancers11030348
4. Biazzo A, De Paolis M. Multidisciplinary approach to osteosarcoma. *Acta Orthop Belg*. 2016;82(4):690–698.
5. Allison DC, Carney SC, Ahlmann ER, et al. A meta-analysis of osteosarcoma outcomes in the modern medical era. *Sarcoma*. 2012;2012:704872. doi:10.1155/2012/704872
6. Wang C, Jing J, Cheng L. Emerging roles of non-coding RNAs in the pathogenesis, diagnosis and prognosis of osteosarcoma. *Invest New Drugs*. 2018;36(6):1116–1132. doi:10.1007/s10637-018-0624-7
7. Bacci G, Briccoli A, Rocca M, et al. Neoadjuvant chemotherapy for osteosarcoma of the extremities with metastases at presentation: recent experience at the Rizzoli Institute in 57 patients treated with cisplatin, doxorubicin, and a high dose methotrexate and ifosfamide. *Ann Oncol*. 2003;14(7):1126–1134. doi:10.1093/annonc/mdg286
8. Boye K, Del Prever AB, Eriksson M, et al. High-dose chemotherapy with stem cell rescue in the primary treatment of metastatic and pelvic osteosarcoma: final results of the ISG/SSG I study. *Pediatr Blood Cancer*. 2014;61(6):840–845. doi:10.1002/pbc.24868
9. Goorin AM, Harris MB, Bernstein M, et al. Phase II/III trial of etoposide and high dose ifosfamide in newly diagnosed metastatic osteosarcoma: a pediatric oncology group trial. *J Clin Oncol*. 2002;20(2):426–433. doi:10.1200/JCO.2002.20.2.426
10. Aljubran AH, Griffin A, Pintilie M, Blackstein M. Osteosarcoma in adolescents and adults: survival analysis with and without lung metastases. *Ann Oncol*. 2009;20(6):1136–1141. doi:10.1093/annonc/mdn731
11. Novelda F, Mayr L, Kubista B, et al. EGFR is not a major driver for osteosarcoma cell growth in vitro but contributes to starvation and chemotherapy resistance. *J Exp Clin Cancer Res*. 2015;34:134. doi:10.1186/s13046-015-0251-5
12. Enomoto K, Fallen S, Abaan HO, et al. Wnt10b induces chemotaxis of osteosarcoma and correlates with reduced survival. *Pediatr Blood Cancer*. 2008;51(3):349–355. doi:10.1002/pbc.21595
13. Zhao S, Kurenbekova L, Gao Y, et al. NKD2, a negative regulator of Wnt signaling, suppresses tumor growth and metastasis in osteosarcoma. *Oncogene*. 2015;34(39):5069–5079. doi:10.1038/onc.2014.429
14. Zhao SJ, Jiang YQ, Xu NW, et al. SPARCL1 suppresses osteosarcoma metastasis and recruits macrophages by activation of canonical WNT/β-catenin signaling through stabilization of the WNT-receptor complex. *Oncogene*. 2018;37(8):1049–1061. doi:10.1038/onc.2017.403
15. Cao J, Wang Y, Dong R, et al. Hypoxia-induced WSB1 promotes the metastatic potential of osteosarcoma cells. *Cancer Res*. 2015;75(22):4839–4851. doi:10.1158/0008-5472.CAN-15-0711
16. Sasaki R, Osaki M, Okada F. MicroRNA-based diagnosis and treatment of metastatic human osteosarcoma. *Cancers (Basel)*. 2019;11(4):553. doi:10.3390/cancers11040553
17. Yang Z, Li X, Yang Y, et al. Long noncoding RNAs in the progression, metastasis, and prognosis of osteosarcoma. *Cell Death Dis*. 2016;7(9):e2389. doi:10.1038/cddis.2016.272
18. Wang C, Ren M, Zhao X, et al. Emerging roles of circular RNAs in osteosarcoma. *Med Sci Monit*. 2018;24:7043–7050. doi:10.12659/MSM.912092
19. Jones KB, Salah Z, Del Mare S, et al. miRNA signatures associate with pathogenesis and progression of osteosarcoma. *Cancer Res*. 2012;72(7):1865–1877. doi:10.1158/0008-5472.CAN-11-2663
20. Yang C, Huang D, Ma C, et al. Identification of pathogenic genes and transcription factors in osteosarcoma. *Pathol Oncol Res*. 2020;26(2):1041–1048. doi:10.1007/s12253-019-00645-w
21. Wu G, Zhang M. A novel risk score model based on eight genes and a nomogram for predicting overall survival of patients with osteosarcoma. *BMC Cancer*. 2020;20(1):456. doi:10.1186/s12885-020-06741-4

22. Sun W, Ma X, Shen J, et al. Bioinformatics analysis of differentially expressed pathways related to the metastatic characteristics of osteosarcoma. *Int J Mol Med*. 2016;38(2):466–474. doi:10.3892/ijmm.2016.2657
23. Wang Z, Lachmann A, Keenan AB, Ma'ayan A, Stegle O. L1000FWD: fireworks visualization of drug-induced transcriptomic signatures. *Bioinformatics*. 2018;34(12):2150–2152. doi:10.1093/bioinformatics/bty060
24. Cotto KC, Wagner AH, Feng YY, et al. DGIdb 3.0: a redesign and expansion of the drug-gene interaction database. *Nucleic Acids Res*. 2018;46(D1):D1068–D1073. doi:10.1093/nar/gkx1143
25. Gao Y, Kim S, Lee YI, Lee J. Cellular stress-modulating drugs can potentially be identified by in silico screening with connectivity map (CMap). *Int J Mol Sci*. 2019;20(22):5601. doi:10.3390/ijms20225601
26. Wu J, Zhang H, Zhang W, et al. Lentivirus-mediated shRNA interference of trefoil factor 3 blocks cell viability, migration and invasion in the papillary thyroid carcinoma cells. *Neoplasma*. 2018;65(2):169–177. doi:10.4149/neo_2018_170119N51
27. Shaikh AB, Li F, Li M, et al. Present advances and future perspectives of molecular targeted therapy for osteosarcoma. *Int J Mol Sci*. 2016;17(4):506. doi:10.3390/ijms17040506
28. Meazza C, Scanagatta P. Metastatic osteosarcoma: a challenging multidisciplinary treatment. *Expert Rev Anticancer Ther*. 2016;16(5):543–556. doi:10.1586/14737140.2016.1168697
29. Perry JA, Kiezun A, Tonzi P, et al. Complementary genomic approaches highlight the PI3K/mTOR pathway as a common vulnerability in osteosarcoma. *Proc Natl Acad Sci U S A*. 2014;111(51):E5564–73. doi:10.1073/pnas.1419260111
30. Isakoff MS, Bielack SS, Meltzer P, Gorlick R. Osteosarcoma: current treatment and a collaborative pathway to success. *J Clin Oncol*. 2015;33(27):3029–3035. doi:10.1200/JCO.2014.59.4895
31. Ferrari S, Serra M. An update on chemotherapy for osteosarcoma. *Expert Opin Pharmacother*. 2015;16(18):2727–2736. doi:10.1517/14656566.2015.1102226
32. Jemal A, Ward EM, Johnson CJ, et al. Annual report to the nation on the status of cancer, 1975–2014, featuring survival. *J Natl Cancer Inst*. 2017;109(9):djx030. doi:10.1093/jnci/djx030
33. Wang W, Zhao HF, Yao TF, Gong H. Advanced development of ErbB family-targeted therapies in osteosarcoma treatment. *Invest New Drugs*. 2019;37(1):175–183. doi:10.1007/s10637-018-0684-8
34. Stokowa-Sołtys K, Barbosa NA, Kasprowicz A, et al. Studies of viomycin, an anti-tuberculosis antibiotic: copper(ii) coordination, DNA degradation and the impact [illegible] ribozyme cleavage activity. *Dalton Trans*. 2016;[illegible](20):8645–[illegible]658. doi:10.1039/C6DT00245E
35. Holm M, Borg A, Ehrenberg M, [illegible]val S. Molec[illegible]r mechanism of viomycin inhibition of pe[illegible]de elonga[illegible]n in bacte[illegible]. *Proc Natl Acad Sci U S A*. 2016;113([illegible]978–983. doi:10.1073/[illegible]as.1517541113